

# Numerical Analysis of Polymer Micro-model Flooding Experiments

Jonas Wegner and Leonhard Ganzer

Institute of Petroleum Engineering, Clausthal University of Technology,  
Agricolastraße 10, 38678 Clausthal-Zellerfeld, Germany

**Abstract.** Adding polymers to the injection water leads to an increase in water viscosity together with a reduction in water permeability. As a result, the mobility ratio improves leading to a more efficient displacement process and a higher oil recovery factor. Different physical and chemical processes accompany the flow of aqueous polymer solutions in porous media resulting in the loss of polymer solution viscosity. The numerical simulation of polymer EOR in porous media relies on mathematical models that have already been proposed in literature. However, direct comparison between numerical simulations and experimental data from flood experiments is limited. Although important parameters can be obtained from core experiments, the local distribution of static and dynamic fluid transport parameters remains largely unknown. 2D micromodels such as silicon edged pore networks are an alternative as they provide visual access to the flooding process and enable a detailed quantification of the local distribution of relevant transport parameters. In this paper, a micromodel simulator that considers polymer related physical and chemical effects such as non-Newtonian rheology of the displacing phase, permeability reduction, retention and salinity effects is presented using comprehensive mathematical models. For the solution of transport system equations the software Matlab<sup>®</sup> by MathWorks, Inc. is used as it provides a flexible framework for implementing the underlying transport and auxiliary equations. A pattern generator code is used to define the 2D micromodel structure, generating predefined porosity and permeability averages with local heterogeneities. These generated patterns lead to the micromodels used in this work.

Results obtained from micromodel flooding experiments will be compared to results from numerical simulation in order to test the ability of existing mathematical models to reproduce dominating physico-chemical effects.

The work aims to provide and support selection criteria for optimizing polymer EOR by predicting polymer performance for a variety of critical input parameters such as polymer selection, polymer concentration, salinity and target viscosity for various average reservoir qualities ( $k$ ,  $\phi$ ).

**Keywords:** micromodel, polymer flooding, simulation, enhanced oil recovery.

## 1 Introduction

The industry standards used to investigate polymer flow in porous media and thus to determine important parameters relevant to polymer EOR projects are core flood experiments. Although important parameters can be gathered from these experiments, the cores remain a “black box” to some extent. However, the distribution of static and dynamic flow properties throughout the flooding process contains valuable information relevant for the design of polymer EOR projects. Compared to cores, micromodels such as silicon edged pore-networks enable visual access to the flooding process. Existing mathematical models can be implemented into a simulator to reproduce different physico-chemical effects observed during experiments.

## 2 Micromodel Design and Experimental Set-Up

### 2.1 *Micromodel Design – “Pattern Generator”*

Prior to building silicon edged micromodels, a digital representation of the desired 2D pore-structure in DXF file format is required. The “Pattern Generator” is a computer program capable of generating artificial pore-networks at a high level of complexity in the required format. Because of its extensibility and the large number of available modules, a hybrid framework of python and Matlab<sup>®</sup> [1] is used for the development of the “Pattern Generator”. Four different patterns have been created on a quadratic domain (20x20x0.02 mm) as depicted in Figure 1:

- a.) A stochastic composition of circles with different radii based on a normal distribution and a fixed porosity.
- b.) A pattern consisting of regular-spaced circles with quadrilaterals between them
- c.) A pattern consisting of regular-spaced circles of the same size.
- d.) A “dual porosity” pattern consisting of diamond-shaped collections representing the matrix and void space between them as well as fracture.

Porosity is determined as the fraction of the void area over the total area. The results are presented in Table 1. The porosity is between 18 % - 27 % for all structures which is representative of real porous media.

### 2.2 *Experimental Set-Up*

A schematic diagram of the experimental flooding set-up used is presented in Figure 2 a).

Polymers are injected with a syringe pump via a multi-port valve into the micromodel holder and into the micromodel. A top view of a micromodel can be found in Figure 2 b). As depicted the micromodel consists of the pore structure, inlet and outlet channels and boreholes. The flooding process is visualized using a fluorescence microscope & camera.

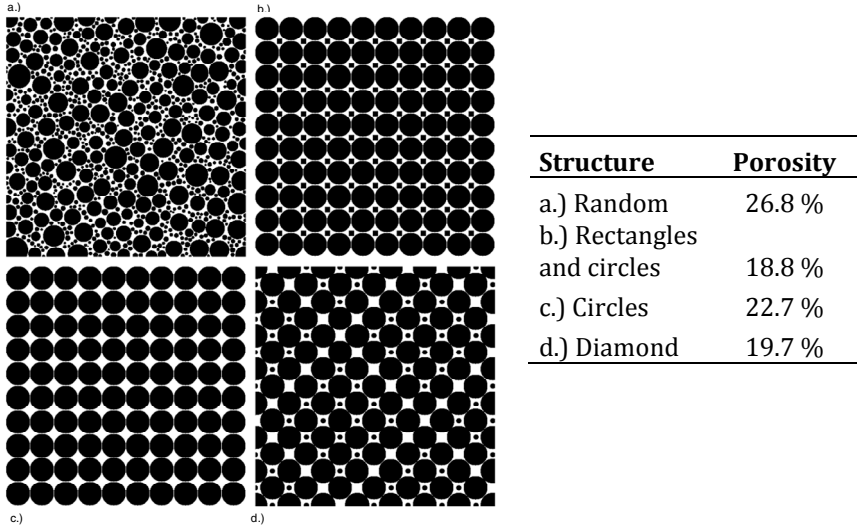


**Fig. 1** Four different example pore-networks (a–d) were generated with the “Pattern Generator”. The original size of a) is 2x2 mm and (c-d) is 5x5 mm.

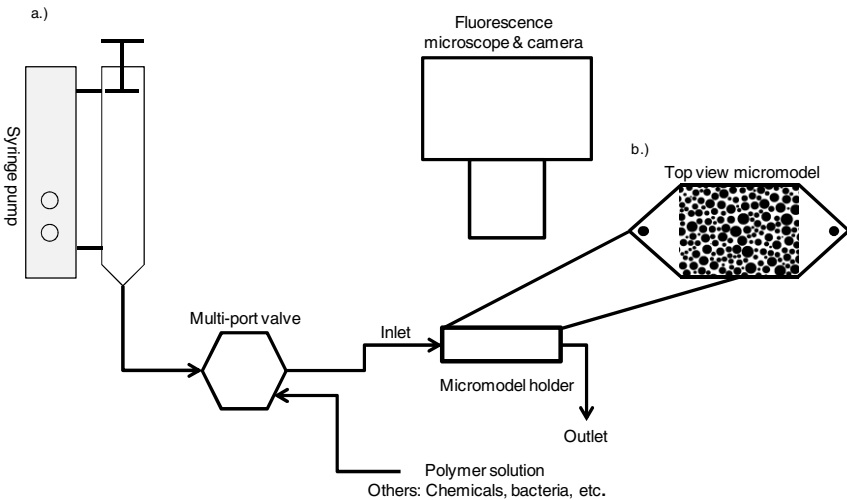


**Fig. 2** a) Schematic diagram of the experimental set-up and b) top view of the micromodel pore-network inlet/outlet channels and boreholes (According to Baumann (2006))

### 3 Micromodel Simulator

A two phase, four-component polymer EOR model is implemented into Matlab® [1] to simulate the displacement of oil by aqueous polymer solutions in micromodels. The oleic phase consists of a single component oil, while the aqueous phase contains the components water, polymer and salt. Although several complex physico-chemical processes influence the flow of aqueous polymer solutions in porous media under in-situ reservoir conditions, the following assumptions and modifications are made for the micromodel experiments considered here:

- a.) The model is two-dimensional, the properties of the porous structure are homogeneous, and gravity is neglected.
- b.) Experiments are conducted at atmospheric temperature and pressure.
- c.) Hence, the oleic and aqueous phases as well as the porous media edged onto the micromodel are assumed to be incompressible.
- d.) Polymer adsorption reduces the relative permeability of the aqueous phase only.
- e.) A Generalization of Darcy's law is applicable to multiphase flow.
- f.) Multicomponent dispersion is neglected.
- g.) Salt is not adsorbed onto the solid surface, but has an impact on the viscosity of the aqueous polymer solution.
- h.) Salt, polymer and water are fully mixed.

#### 3.1 Flow Equations

Taking into account the above assumptions, the simultaneous flow of two immiscible fluid phases in porous media can be described by the mass conservation equation for each phase. For the aqueous phase this is written as:

$$\frac{\partial(\phi S_a)}{\partial t} = \nabla \cdot \left( \frac{k_a}{\mu_a} \nabla p_a \right) + \tilde{q}_a \quad (1)$$

The mass conservation equation for the oleic phase is:

$$\frac{\partial(\phi S_o)}{\partial t} = \nabla \cdot \left( \frac{k_o}{\mu_o} \nabla p_o \right) + \tilde{q}_o, \quad (2)$$

where  $p$ ,  $\mu$ ,  $S$ ,  $k$ ,  $\phi$  are the pressure, viscosity, saturation, effective permeability and porosity of the porous media. The subscripts  $o$  and  $a$  represent the oleic and aqueous phases, respectively.  $\tilde{q}$  is the source/sink term.

The fact that the void space of the porous media is completely filled with the oleic and aqueous phase, leads to the following relation:

$$S_a + S_o = 1 \quad (3)$$

### 3.2 Transport Equations

Polymer and salt are converted with the bulk Darcy velocity of the aqueous phase. For both salt and polymer, a transport equation is required. The equation for polymer transport is written as:

$$\frac{\partial(\phi S_a C_p)}{\partial t} + \frac{\partial(A_v C_{pad})}{\partial t} = \nabla \cdot \left( C_p \frac{k_a}{\mu_a} \nabla p_a \right) + \tilde{q}_a C_{pw} \quad (4)$$

The equation for salt transport is written as:

$$\frac{\partial(\phi S_a C_s)}{\partial t} = \nabla \cdot \left( C_s \frac{k_a}{\mu_a} \nabla p_a \right) + \tilde{q}_a C_{sw}, \quad (5)$$

where  $C$ ,  $A_v$  are the component concentrations on a specific surface area of the micromodel. The subscripts  $p$ ,  $s$  represent the polymer and salt components, respectively.  $C_{pw}$  and  $C_{sw}$  are the polymer and salt concentrations at the injection boundary.  $C_{pad}$  is the mass of polymer adsorbed per unit mass of rock. Due to adsorption of polymer on the rock-fluid interface, physical parameters such as the rock permeability change. In addition to adsorption, non-Newtonian rheology and salinity effects have an impact on the aqueous phase viscosity. Therefore, additional constitutive equations are required to close and couple the system of equations (1) – (5).

### 3.3 Cross Couplings

#### 3.3.1 Salinity and Concentration Effects

The viscosity of the polymer solution at “zero” shear rate depends on the salt as well as polymer concentration. A mathematical relation describing the dependence of the aqueous phase viscosity on polymer and salt concentration is the Flory-Huggins equation [3].

$$\mu_a^0 = \mu_w \cdot \left( 1 + (a_1 C_p + a_2 C_p^2 + a_3 C_p^3) \cdot C_s^{Sp} \right) \quad (6)$$

where  $a_1, a_2, a_3$ , and  $S_p$  are fitting constants. The units of the fitting constants are selected such that the items in the parenthesis become dimensionless.

### 3.3.2 Polymer Adsorption

Polymer adsorption causes a reduction of polymer concentration in the aqueous phase, hence, a reduction in aqueous phase viscosity. The degree of polymer adsorption depends on the type of polymer and rock, but in general it increases with higher polymer concentrations. The relation between the concentration of polymer in the aqueous phase and the concentration of polymer in the adsorbed state is described by the Langmuir isotherm [4].

$$\frac{C_{pad}}{C_{pad}^{\max}} = \frac{bC_p}{1 + bC_p}, \quad (7)$$

Where  $b$  is a Langmuir constant and  $C_{pad}^{\max}$  is the maximum polymer concentration adsorbed to the rock. Adsorption can be considered reversible or irreversible. The Langmuir isotherm presented here is an equilibrium relation and cannot be used directly if the adsorption is irreversible. In such a case, the maximum adsorption must be traced for each time step.

$$C_{pad}^{\max} = \max\left\{(C_{pad})^1, (C_{pad})^2, \dots, (C_{pad})^n\right\} \quad (8)$$

### 3.3.3 Permeability Reduction Factor

As a result of polymer adsorption on the rock surfaces, the permeability of the aqueous phase is reduced while the permeability of the oelic phase is unaltered. The permeability reduction factor representing the effect of polymer adsorption on the permeability of the aqueous phase is defined as  $R_k = k_w / k_a$ , where  $k_w$  is the water permeability. Further the permeability reduction factor can be expressed as [5]:

$$R_k = 1 + (R_{RF} - 1) \frac{C_{pad}}{C_{pad}^{\max}}, \quad (9)$$

where  $R_{RF}$  is the residual resistance factor. It represents the decrease in rock permeability when the maximum amount of polymer is adsorbed [1].

### 3.3.4 Non-Newtonian Rheology

The aqueous polymer solution behaves like a non-Newtonian fluid. Then, the following relation can be defined where shear rate and viscosity apply in the Carreau equation [6].

$$\mu_a - \mu_\infty = (\mu_{a0} - \mu_\infty) \cdot \left[1 + (\lambda \dot{\gamma}_{eq})^\alpha\right]^{(n-1)/\alpha} \quad (10)$$

Where,  $\mu_\infty$  and  $\mu_a$ , are the water and aqueous phase viscosity, respectively.  $\lambda$ ,  $\alpha$ ,  $n$  are polymer specific constants and  $\dot{\gamma}_{eq}$  is the equivalent shear rate in the porous media. A relation to calculate the apparent shear rate exerted on polymers while flowing through porous media is given by [7]:

$$\dot{\gamma}_{eq} = C \left[ \frac{(3n+1)}{4n} \right]^{n/(n-1)} \cdot \left[ \frac{u_w}{\sqrt{\bar{k} k_{rw} S_w \phi / R_{RF}}} \right] \quad (11)$$

Where,  $C$  is a constant,  $\bar{k}$  is an average permeability and  $u_w$  is the water velocity.

### 3.3.5 Saturation, Capillary Pressure and Relative Permeability

In order to solve the two-phase flow problem (Eqs. 1 to 3), three additional constitutive equations need to be specified. Due to the curvature and surface tension of the interface between the phases, the pressure in the wetting phase is less than in the non-wetting phase. The pressure difference is defined by the capillary pressure  $p_c$ , which is expressed as [8]:

$$p_c(S_a) = p_o - p_a \quad (13)$$

In this model, we used the following capillary pressure model [8]:

$$p_c = p_t \cdot S_n^{\frac{1}{\phi}}, \quad (14)$$

where  $\phi$ ,  $p_t$  are the Brooks-Corey coefficient and the capillary entry pressure and  $S_n$  is the normalized water saturation defined as [8]:

$$S_n = \frac{S_a - S_{ra}}{1 - S_{ra} - S_{ro}}, \quad (15)$$

$S_{ra}$  and  $S_{ro}$  are the residual and immobile saturations of the aqueous and oleic phases. The effective permeabilities of water  $k_{rw}$  and the oleic phase  $k_{ro}$  are calculated using the Brooks-Corey correlation [8].

$$k_a = \frac{k \cdot S_n^{\frac{2+3\phi}{\phi}}}{R_k} = \frac{k \cdot k_{rw}}{R_k} \quad (16)$$

$$k_o = k \cdot (1 - S_n)^2 \left( 1 - S_n^{\frac{2+\phi}{\phi}} \right) = k \cdot k_{ro}$$

## 4 Model Parameterization and Fluid Properties

### 4.1 Micromodel Geometry

Figure 3 shows a microscopic image of the regular circled structure depicted in Figure 1 c) edged onto a silicon wafer. The size of the pore structure is 20 x 20 mm. Inlet/outlet boreholes appear black. Two fans are used to transport fluids from the inlet/outlet borehole to the porous structure. This approach flow concept was selected to establish linear flow conditions which are favorable for the Measurement of single phase flow properties of the structure. The porosity of the pore structure obtained from the pattern generator is 22.

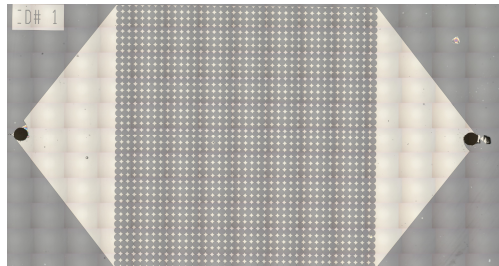


Fig. 3 Top view of the micromodel used in the experiment

### 4.2 Micromodel Permeability

The permeability of the micromodel is determined by the following procedure. First, the micromodel is flooded with CO<sub>2</sub> to displace the remaining air. As all the CO<sub>2</sub> is dissolved in the water and 100 % water saturation is established, the pressure differential is measured at different injection rates. Based on Darcy's law the permeability can be calculated. The measurements show micromodel permeability of 480 mD which will be used in the numerical simulations.

### 4.3 Fluid Properties

The viscosity of the water with 1 % NaCl used at 25 °C is 1.1 cP and is constant for different shear rates. An aqueous polymer solution is a non-Newtonian fluid. Polymer X, with high temperature and salinity resistant characteristics has been used for the experiments.

The rheology was measured at 25 °C with a salt concentration of 1 % NaCl using the Kinexus pro Rheometer by Malvern [9]. Prior to the measurement the aqueous polymer solution was filtered through a 1.2 micron screen. The results are shown in Figure 4. Based on the bulk rheological measurements the following constants described previously  $S_p$ ,  $a_1$ ,  $a_2$ ,  $a_3$ ,  $\lambda$ ,  $\alpha$  and  $n$  can be determined. All parameters used to populate the simulation model are summarized in Table 1. Where no experimental data is available, parameters are assumed.



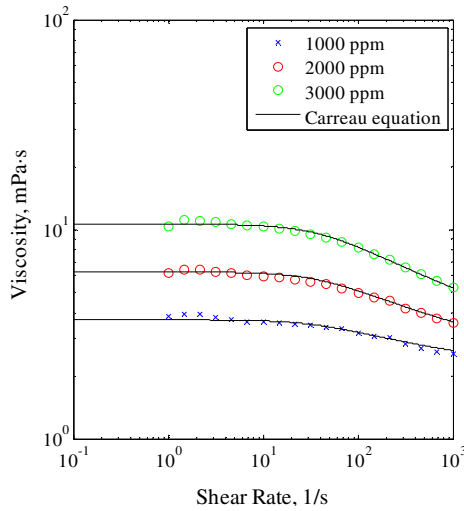


**Fig. 4** Rheology of the X polymer for different polymer concentrations, 1% NaCl and 25 °C

**Table 1** Physical parameters used as input in simulation

Physical parameter	Value	Physical parameter	Value
Length, $x$ (cm)	2	Water viscosity, $\mu_w$ (mPa·s)	1.1
Width, $y$ (cm)	2	Specific surface area, $A_v$ (1/cm)	160
Height, $z$ (cm)	20E-4	Langmuir adsorption constant, $b$ (cm <sup>3</sup> /mg)	10
Gridblock size, $\Delta x, \Delta y$ (cm)	0.01	Maximum adsorption, $C_{pad}^{max}$ (mg/cm <sup>2</sup> )	8.4E-4
Porosity, $\phi$	0.23	Permeability, $k$ (mD)	480
Init. salt concentration, $c_s$ (mg/cm <sup>3</sup> )	10	Shear rate exponent, $n$	0.82
Constant, $\lambda$ (s)	1/25	Constant, $c$	1
Residual resistance factor, $R_{RF}$	2	Constant, $\alpha$	2
Injection Rate, $Q$ (cm <sup>3</sup> /h)	0.0032	Constant, $a_1, a_2, a_3$ (-)	5, 0.4, 0
Polymer inj. concentration, $Q_{pw}$ (mg/cm <sup>3</sup> )	1 (5 min) 0 (25 min)	Constant, $s_p$	-0.414

## 5 Numerical Simulations

In order to generate results, the physical parameters presented in Table 1 are used in the simulator implemented into Matlab® [1]. Simulation results of the polymer concentration after 5 minutes are presented in Figure 5. In the case of heterogeneous and anisotropic permeability field, viscous fingering occurs as shown in Figure 5a. In the case presented here, the micromodel permeability is 480 mD and homogeneous and isotropic (Figure 5 b)), and a 1D representation of the results is sufficient.

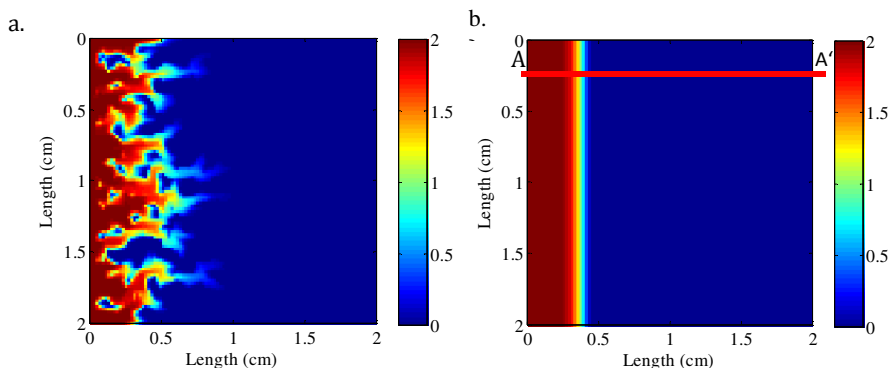


**Fig. 5** Polymer concentration in mg/cm<sup>3</sup> after 5 minutes of polymer injection for a) a heterogeneous/anisotropic and b) homogeneous /isotropic case

The simulation results are presented in Figure 6 and are plotted along the cross section A-A' (Figure 5 b). During the first 5 minutes a polymer slug with a concentration of 2 mg/cm<sup>3</sup> is injected into the micromodel (Figure 6 a.)). After 5 minutes the slug is displaced by water. The salt concentration is 10 mg/cm<sup>3</sup> and constant. Due to adsorption the size of the polymer slug is reduced to a maximum concentration of 1.5 mg/cm<sup>3</sup> after 25 minutes (Figure 6 a.)). As the polymer adsorption is assumed irreversible, no desorption occurs although polymer concentration decreases (Figure 6 b)).

Further, the permeability to the aqueous phase is reduced as can be seen in Figure 6 c) which is a result of polymer retention. Due to adsorption and shear thinning, the viscosity of the aqueous phase is slightly reduced (Figure 6 d)). The apparent shear rate depends on the level of adsorption and is between 7-10 1/s. Figure 6 d) depicts that in this case the viscosity alteration caused by shear thinning is small.

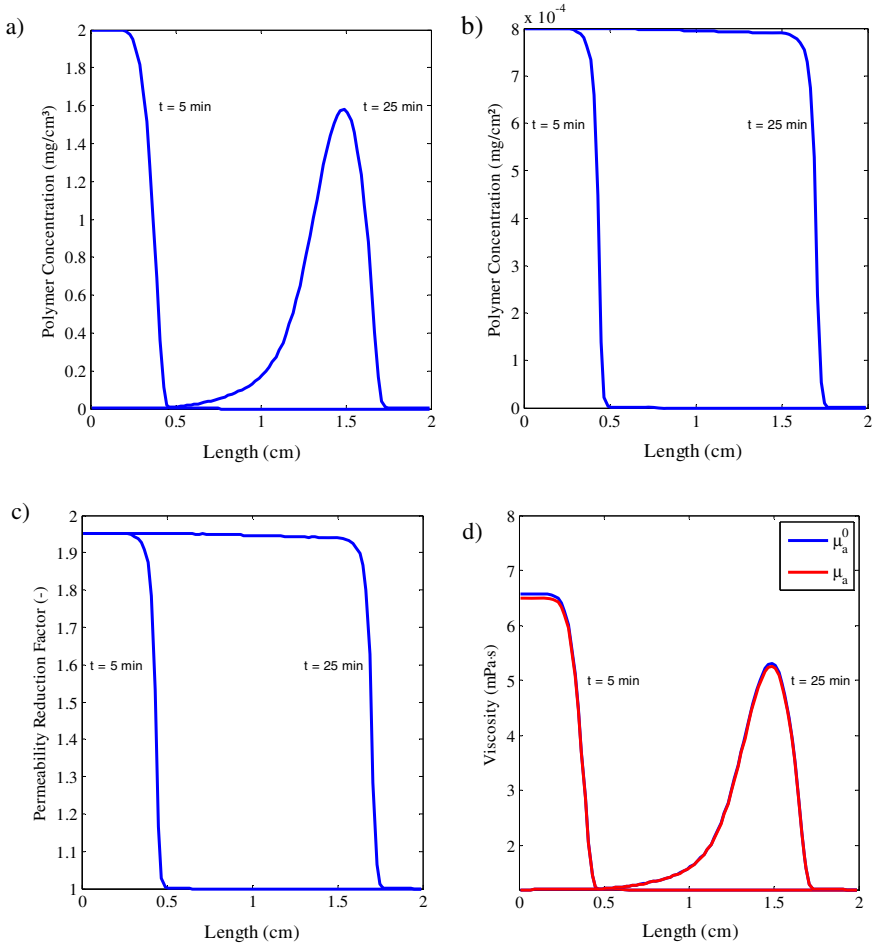


**Fig. 6** Simulation results of a) Polymer concentration, adsorbed polymer concentration, c) permeability reduction factor and d) aqueous phase viscosity with and without shear

## 6 Conclusions

- (1) The implementation of a comprehensive mathematical polymer flood model has been presented. It considers different physico-chemical effects such as non-Newtonian rheology of the displacing phase, permeability reduction, retention and salinity effects by using comprehensive mathematical models.
- (2) The micromodel properties such as porosity and permeability as well as fluid properties have been determined experimentally. Where parameters were not determined experimentally they are assumed.
- (3) Polymer X with 1 % NaCl and a homogeneous and isotropic micomodel was used. Rheology was determined experimentally.

- (4) The simulation results show, that the impact of shear on the apparent viscosity of the aqueous phase is small compared to the effect of polymer concentration. This is the result of the polymer type and low shear rates encountered. A shear rate between 7-10 1/s was simulated.

## 7 Outlook

Results obtained from the two phase micromodel flooding experiments will be compared with the results from numerical simulation in order to test the ability of existing mathematical models to reproduce dominating physico-chemical effects. Further, parameters such as adsorption isotherm, residual resistance factor, and parameters affecting apparent shear rate will be determined experimentally and will be used in simulation. This will establish a more detailed description of the micromodel properties.

## References

1. Matlab® The Language of Technical Computing by The MathWorks, Inc., <http://www.mathworks.de/>
2. Baumann, T., Niessner, R.: Micromodel study on reparationing phenomena of a strongly hydrophobic fluorophore at colloid/1-octanol interface. *Water Resources Research* 42, 12 (2006), doi:10.1029/2006WR004893
3. Flory, P.J.: *Principles of Polymer Chemistry*. Cornell University Press (1953)
4. Lakatos, I., Lakatos-Szabo, J., Toth, J.: Factors influencing polyacrylamide adsorption in porous media and their effect on flow behavior. Paper presented at the Symposium on Surface Phenomena in EOR, Stockholm (1989)
5. Islam, M., Farouq, S.: New scaling criteria for polymer emulsion and foam flooding experiments. *J. Can. Petrol Technol.* 28(4), 79–87 (1989)
6. Hirasaki, G.J., Pope, G.A.: Analysis of factors influencing mobility and adsorption in the flow of polymer solution through porous media. *SPEJ*, 337–346 (August 1974)
7. Carreau, P.J.: *Rheological Equations from Molecular Network Theories*. *Trans. Soc. Rheol.* 16(1), 99–127 (1972) (Ph.D. dissertation, University of Wisconsin, Madison, 1968)
8. Brooks, R., Corey, A.: *Hydraulic Properties of Porous Media*. In: *Colorado State University Hydrology Paper*, vol. 3, Colorado State University (1964)
9. © 2012- Malvern Instruments Ltd. a Spectris company (2012), <http://www.malvern.de>